# Raman solitons with group velocity dispersion

D. V. Skryabin and A. V. Yulin
*Centre for Photonics and Photonic Materials, Department of Physics, University of Bath, Bath BA2 7AY, United Kingdom*
(Received 31 July 2006; published 25 October 2006)

We consider the coupled propagation of the pump and Stokes waves in a Raman active medium accounting for the group velocity walk off and group velocity dispersion. Interplay of the Raman coherence and the dispersion can lead to the formation of a complete band gap in the spectrum of linear waves consisting of the two consecutive subgaps located at different frequencies. Using an approximate analytic technique, we find exponentially localized solitons residing in the complete gap, and find algebraic solitons when the gap is closed. Feasibility of observation of these structures in hollow fibers is discussed.

DOI: 10.1103/PhysRevE.74.046616 PACS number(s): 42.65.Tg, 42.50.Gy, 42.65.Dr, 42.50.Md

## I. INTRODUCTION

Solitons in a coupled system of Maxwell and Schrödinger equations represent a physically distinct alternative to solitons in systems where nonlinear corrections to the refractive index are derived as Taylor expansions in the field products. Slow light in coherent atomic systems having applications to quantum processing of information [1] and generation of the ultrashort pulse trains in a Raman medium [2] are both related to the certain classes of the solitonic solutions [3–5] of the Maxwell-Schrödinger system, often referred to as Maxwell-Bloch equations. Availability of recently developed photonic band-gap (PBG) fibers with the gas filled hollow cores allows to carry out quantum optics experiments [6–8] in low loss, tightly focused and, simultaneously, diffraction free regimes. These factors create favorable conditions for the soliton related experiments [9] and have been shown to dramatically reduce thresholds for the cascaded Raman process and electromagnetically induced transparency [7,8].

PBG fibers, however, poses noticeable Kerr nonlinearity and strong geometrical dispersion, which are intrinsically linked to the fiber structure. In our recent work [10] we have confirmed that the Raman solitons in the Maxwell-Schrödinger system withstand presence of the Kerr nonlinearity, which, however, influences their stability properties. Our estimates [10] have demonstrated that typical durations of the Raman solitons can vary from a few pico-seconds to 100s of femtoseconds. For such pulse durations the group velocity dispersion (GVD) resulting from the combination of the waveguide dispersion and dispersion due to non-Raman transitions in the gas are expected to be of importance. The aim of this work is to analyze GVD effects on Raman solitons. We demonstrate that the Raman system with GVD terms allows substantial analytical advances to be made in certain limits and the problem is interesting enough to study it separately from other complications. Observation of the Raman solitons still represents a challenge and we hope that continuing theoretical studies will stimulate experimental activities.

## II. MODEL EQUATIONS AND PREVIOUS RESULTS

We consider the propagation of the two optical pulses with the envelopes described by the functions $\tilde{B}_{1,2}(z,\tau)$ with the carrier frequencies $\omega_1 > \omega_2$, such that $\omega_1 - \omega_2 = \omega_R$ is the Raman transition frequency. Using the slowly varying envelope approximation for the optical fields and the rotating wave approximation for the antidiagonal elements of the density matrix, one can derive the following dimensionless system, see [11] and the Appendix below, where the derivation and normalization procedures are described in detail:

$$i[\partial_z + s\partial_\tau + id_1\partial_\tau^2]\tilde{B}_1 = -Q\tilde{B}_2, \tag{1}$$

$$i[\partial_z - s\partial_\tau + id_2\partial_\tau^2]\tilde{B}_2 = -Q^*\tilde{B}_1, \tag{2}$$

$$i\partial_\tau Q = -\tilde{B}_1\tilde{B}_2^*\sigma, \tag{3}$$

$$\partial_\tau \sigma = -\frac{i}{2}[\tilde{B}_1\tilde{B}_2^*Q^* - \tilde{B}_1^*\tilde{B}_2 Q]. \tag{4}$$

Here $Q$ is the Raman coherence and $\sigma$ is the population inversion. $Q=0$ and $\sigma=1$ correspond to the unexcited Raman medium. Relaxation of $Q$ and $\sigma$ has been disregarded under the assumption of the sufficiently short pulse durations (see the Appendix). The equality

$$\sigma^2 + |Q|^2 = 1, \tag{5}$$

can be derived from the condition that the total population of the levels is 1. If the physical time is normalized to the characteristic walk-off time of the two fields, then $|s|=1$ (see the Appendix). Without restriction of generality we can assume $s=-1$. Parameters $d_{1,2}$ measure the ratio of the walk-off length to the GVD length. Physical scales involved for a typical PBG filled with $D_2$ are such that one unit of $\tau$ approximately corresponds to 200 fs, unit of $z$—to 0.6 cm, unit of $|B_{1,2}|^2$—to $4\times10^{12}$ W/cm$^2$, and $|d_{1,2}|$ can vary from zero to $\sim 0.1$ (see the Appendix for details). The above power levels are well within the reach of the amplified short-pulsed laser systems.

Previous theoretical studies of the pulse propagation and solitons in Raman media can be divided into two groups. The first group deals with the classical model, when the medium is described by the classical oscillator equation, which is Eq. (3) with $\sigma=1$. This approximation is valid for weak excitations only, when most of the population remains in the ground state. Solitons and other types of the localized solu-

 

tions in this model have been reported in many studies, see, e.g., [12]. Inclusion of GVD effects into this model together with large detunings from the Raman resonance enable existence of the nonlinear Schrödinger (NLS) type bright-bright, dark-bright, and dark-dark soliton pairs [13]. While, the GVD effects for $\sigma$ constrained to 1 lead to the NLS type of solitons [13], $\sigma \neq 1$ allows for the stationary values of $|Q|$ different from 0 and therefore creates conditions for the gap solitons to exist, see Ref. [10] and below.

Raman solitons in the model accounting for the dynamics of $\sigma$ have been first reported in [14] for the two-field case and later generalized to the multifrequency case [3]. This model has been extensively used for backing of the experimental work on generation of the short pulses in the cascaded Raman process [2], which can be considered as its main experimental test so far. Cascaded excitation of the higher order Raman side bands not accounted for in our model can be suppressed if the fields $\tilde{B}_{1,2}$ are circularly polarized in opposite directions [15]. Integrability properties of the two-field Raman systems have been studied in Ref. [16].

## III. BAND GAPS INDUCED BY THE RAMAN COHERENCE

In what follows we will be seeking the coupled solitons moving with the common group velocity characterized by the parameter $v$ and having the wave number shift $\kappa$. Therefore we assume $\tilde{B}_{1,2}(\tau,z)=B_{1,2}(t=\tau-vz,z)e^{i\kappa z}$ and find

$$i[\partial_z + i\kappa + v_1\partial_t + id_1\partial_t^2]B_1 = -QB_2, \tag{6}$$

$$i[\partial_z + i\kappa + v_2\partial_t + id_2\partial_t^2]B_2 = -Q^*B_1, \tag{7}$$

$$i\partial_t Q = -B_1B_2^*\sigma, \tag{8}$$

$$\partial_t \sigma = -\frac{i}{2}[B_1B_2^*Q^* - B_1^*B_2Q], \tag{9}$$

where

$$v_{1,2} = \mp 1 - v. \tag{10}$$

First we consider properties of the linear wave solutions of Eqs. (6) and (7). Replacing $B_{1,2}$ with $e^{-i\omega t}$ and assuming $Q=0$, we find for the wave numbers $\kappa=v_1\omega+d_1\omega^2$ and $\kappa=v_2\omega+d_2\omega^2$. The dispersion curves intersect at $\omega=0$ and $\omega=\omega_0$, where

$$\omega_0 = \frac{2}{d_1 - d_2}. \tag{11}$$

Finite values of the Raman coherence $Q$ replace crossings of the dispersion curves with the avoided crossings, see Figs. 1(a) and 1(b), forming the two subgaps at $\omega=0$ and $\omega=\omega_0$. Methods of preparation of the finite coherence in the Raman medium have been discussed, e.g., in Ref. [17]. If $d_{1,2}$ have the same signs, then the values of $\kappa$ for the two branches of the dispersion characteristic also have the same signs for $|\omega| \to \infty$. Therefore, the avoided crossings in this case never can form a complete band gap, see Fig. 1(a). Under the complete band gap we understand such a region in the $(\kappa,\omega)$ plane, that one can fit a family of straight lines into it without crossing or touching the dispersion characteristics. If $d_{1,2}$ have the opposite signs, $d_1d_2<0$, then the complete band gap exists, see Fig. 1(b), and it looks like a superposition of the two subgaps separated by $\omega_0$. A typical transmission window of PBG fibers contains the zero GVD point, thereby allowing for the opposite GVD signs of the interacting Raman harmonics. If $d_{1,2}=0$, then there is only one crossing point at $\omega=0$ and one band gap centered at $\omega=0$ [10]. In what follows it is convenient for us to write $d_2$ as follows:

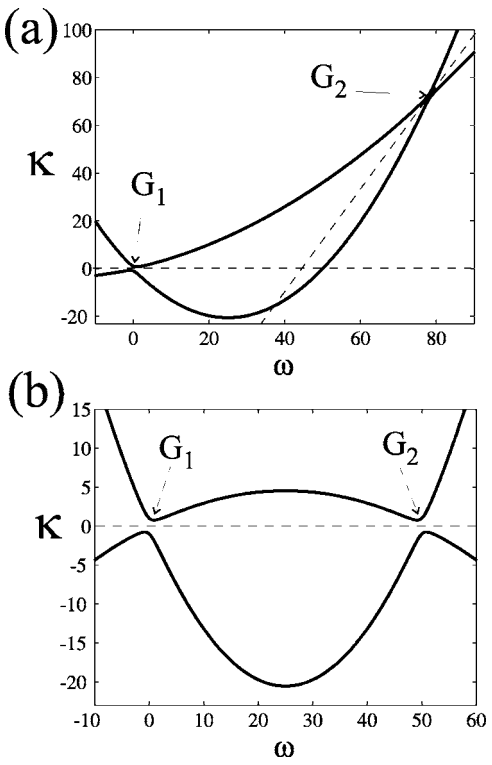


FIG. 1. Dispersion characteristics for $d_1d_2>0$ (a) and $d_1d_2<0$ (b). The parameters are the following: $v_1=-0.36$, $d_1=-0.0072$, $v_2=1.64$, $d_2=-0.0328$ (a) and $v_1=-0.36$, $d_1=0.0072$, $v_2=1.64$, $d_2=-0.0328$. Subgaps $G_{1,2}$ form a complete band gap in the (b) case.

$$d_2 = -d_1 + \epsilon, \tag{12}$$

where $\epsilon$ is a number such that, $d_1d_2<0$, i.e., $d_1\epsilon<d_1^2$.

Dispersion characteristics of the type similar to Fig. 1(b) and corresponding soliton structures have been reported previously quite differently from our contexts of the coupled Korteweg-de Vries equations [18] and coupled LC circuits [19].

## IV. EQUATIONS FOR THE SLOW AMPLITUDES

We demonstrate below that the approximate analytical soliton solutions of Eqs. (6)–(9) can be found in the limit, when $|\omega_0|$ is much greater than the spectral width of the pulses located at the individual subgaps. On the other hand, Eqs. (6) and (7) are already equations for slowly varying

amplitudes and one should assume that the spectral separation of the two subgaps, is less than the Raman frequency. A quantitative criterion for this condition can be chosen as $|\omega_0/\omega_R|<1/2$, where $\omega_{0,R}$ are assumed dimensionless (see the Appendix for numerical estimates).

We assume that $B_1$ and $B_2$ are composed of the two spectral components centered at $\omega=0$ and $\omega=\omega_0$:

$$B_{1,2}=C_{1,2}+G_{1,2}e^{-i\omega_0 t+iKz}. \tag{13}$$

$C_{1,2}$ and $G_{1,2}$ are the functions which vary in $t$ slowly relative to $e^{-i\omega_0 t}$, so that their second derivatives and all the fast oscillating exponential terms can be neglected. The free parameter $K$ characterizes the possible difference of the wave numbers.

Substituting Eq. (13) into Eqs. (6)–(9) we find

$$i[\partial_z+i\kappa+v_1\partial_t]C_1=-QC_2, \tag{14}$$

$$i[\partial_z+i\kappa+v_2\partial_t]C_2=-Q^*C_1, \tag{15}$$

$$i[\partial_z+i(\kappa+\delta)+u_1\partial_t]G_1=-QG_2, \tag{16}$$

$$i[\partial_z+i(\kappa+\delta)+u_2\partial_t]G_2=-Q^*G_1, \tag{17}$$

$$i\partial_t Q=-\sigma(C_1C_2^*+G_1G_2^*), \tag{18}$$

$$\partial_t\sigma=-\mathrm{Im}[Q(C_2C_1^*+G_1^*G_2)], \tag{19}$$

where

$$\delta=K-K_0, K_0=\omega_0\frac{v_1d_2-d_1v_2}{d_2-d_1}, \tag{20}$$

$$u_1=\frac{1+\epsilon/2d_1}{1-\epsilon/2d_1}-v, \quad u_2=-\frac{1-3\epsilon/2d_1}{1-\epsilon/2d_1}-v. \tag{21}$$

In what follows we choose $K=K_0$ implying

$$\delta=0. \tag{22}$$

Formally expansions similar to (13) should be done for $Q$ and $\sigma$. However, higher harmonics of $Q$ and $\sigma$ are of the order of $1/\omega_0$ at least and, we verified numerically that their effect on the results presented below is negligible.

## V. ANALYTICAL SOLITON SOLUTIONS

Now we make a simplifying assumption that all the slow amplitudes can be presented as a constant multiplied by the unknown function $f(x)$, where

$$x=\frac{t}{w} \tag{23}$$

and $w$ is the soliton width, so that

$$C_1=c_1f(x), \quad C_2=ic_2f(x), \tag{24}$$

$$G_1=g_1f(x), \quad G_2(t)=ig_2f(x). \tag{25}$$

We also assume

$$Q=-i\kappa+q(x), \quad \mathrm{Im}\,q=0. \tag{26}$$

Implementing the above substitutions we find that Eqs. (14)–(17) are transformed to

$$i\kappa(c_2-c_1)f=\frac{v_1c_1}{w}\partial_x f+c_2qf, \tag{27}$$

$$i\kappa(c_1-c_2)f=\frac{v_2c_2}{w}\partial_x f-c_1qf, \tag{28}$$

$$i\kappa(g_2-g_1)f=\frac{u_1g_1}{w}\partial_x f+g_2qf, \tag{29}$$

$$i\kappa(g_1-g_2)f=\frac{u_2g_2}{w}\partial_x f-g_1qf. \tag{30}$$

Below we specify two cases when the above system of the differential-algebraic equations has soliton solutions. These cases emerge from the two different constraints leading to the left-hand sides of Eqs. (27) and (28) being zero.

### A. Solutions parametrized by velocity $v$

First we assume $\kappa=0$ and require

$$\partial_x f=qf. \tag{31}$$

This replaces Eqs. (27)–(30) with the two systems of the linear algebraic equations

$$\hat{A}_1\vec{c}=0, \quad \vec{c}=\begin{pmatrix}c_1\\c_2\end{pmatrix}, \quad \hat{A}_1=\begin{pmatrix}\frac{v_1}{w} & 1\\ -1 & \frac{v_2}{w}\end{pmatrix}, \tag{32}$$

$$\hat{A}_2\vec{g}=0, \quad \vec{g}=\begin{pmatrix}g_1\\g_2\end{pmatrix}, \quad \hat{A}_2=\begin{pmatrix}\frac{u_1}{w} & 1\\ -1 & \frac{u_2}{w}\end{pmatrix}. \tag{33}$$

Solvability conditions of these systems are $\det\hat{A}_1=v_1v_2/w^2+1=0$, $\det\hat{A}_2=u_1u_2/w^2+1=0$ and the compatibility condition is $v_1v_2=u_1u_2$. The pulse width $w$ is found from the solvability conditions:

$$w=\sqrt{-v_1v_2}=\sqrt{1-v^2}, \tag{34}$$

$w$ is real providing $v\in(-1,1)$. Compatibility is satisfied providing $1=\alpha_1\alpha_2+v(\alpha_1-\alpha_2)$, where $\alpha_1=\frac{1+\epsilon/2d_1}{1-\epsilon/2d_1}$, $\alpha_2=\frac{1-3\epsilon/2d_1}{1-\epsilon/2d_1}$, see, Eq. (21). If $\epsilon=0$, then $\alpha_{1,2}=1$ and $v$ remains free to vary within its limits. If $\epsilon\neq0$, then the compatibility requires $v=(1-\alpha_1\alpha_2)/(\alpha_1-\alpha_2)$.

In order to avoid unnecessary complications of the notations we will assume below that $v_1<0$ and $u_1>0$. If $\epsilon$ is sufficiently small, then the latter inequality naturally follows from the former, see Eqs. (12) and (21). For the chosen signs the solutions for the constant amplitudes are

$$\frac{c_1}{c_2} = \sqrt{\frac{|v_2|}{|v_1|}}, \quad \frac{g_1}{g_2} = -\sqrt{\frac{|u_2|}{|u_1|}}. \tag{35}$$

Differential equation (31) is complemented by the two equations for $q$ and $\sigma$,

$$\partial_x q = \gamma\sigma f^2, \quad \partial_x \sigma = -\gamma q f^2, \tag{36}$$

where $\gamma = w(c_1c_2 + g_1g_2)$. Now we are implementing a standard substitution

$$q = \sin\phi, \quad \sigma = \cos\phi \tag{37}$$

complying with the probability constraint (5) and valid for $\kappa = 0$. The resulting equations for $\phi$ and $f$ are

$$\partial_x f = f\sin\phi, \quad \partial_x \phi = \gamma f^2. \tag{38}$$

One can show that the above two equations conserve the integral

$$\gamma f^2 + 2\cos\phi = \mathcal{I}_1 = \text{const}. \tag{39}$$

The choice of the integration constant $\mathcal{I}_1$ is physically important and leads to two different types of solutions. We will be seeking for bright soliton solutions, i.e.,

$$\lim_{|t|\to\infty} f = 0. \tag{40}$$

For the initially unexcited medium we have

$$\lim_{|t|\to\infty} \sigma = 1, \quad \lim_{|t|\to\infty} |Q| = 0, \tag{41}$$

which implies $\mathcal{I}_1 = 2$. For the medium initially excited to its maximal coherence we have

$$\lim_{|t|\to\infty} \sigma = 0, \quad \lim_{|t|\to\infty} |Q| = 1, \tag{42}$$

implying $\mathcal{I}_1 = 0$.

#### 1. Solitons with exponentially decaying tails

For the maximum coherence condition (42) the second of the Eqs. (38) transforms to the integrable equation $\partial_x\phi = -2\cos\phi$ giving

$$\cos\phi = -\operatorname{sech}(2x) = \sigma, \tag{43}$$

$$\sin\phi = -th(2x) = Q, \tag{44}$$

$$f^2 = \frac{2}{\gamma}\operatorname{sech}(2x). \tag{45}$$

Each of the systems (32) and (33) is solved up to an arbitrary constant. For example, $c_1$ and $g_2$ can be chosen as arbitrary. After combining Eqs. (24), (25), (36), and (45) one can demonstrate that the final expressions for the field amplitudes depend only on the single arbitrary constant $R = (g_2^2/c_1^2)\sqrt{|u_2v_2|/|u_1v_1|}$:

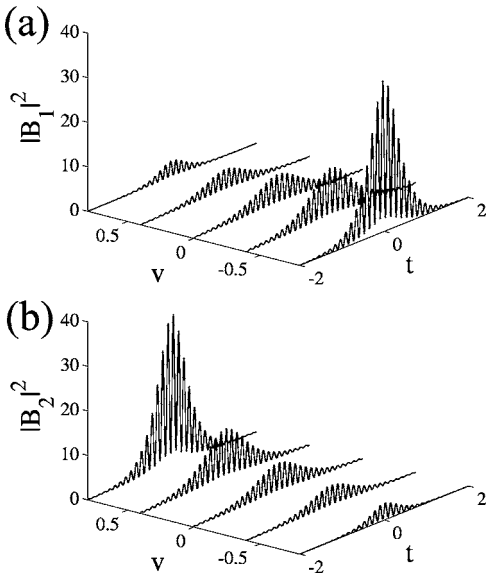


FIG. 2. Intensities $|B_{1,2}(t)|^2$ of the exponentially localized solitons for different values of $v$. The other parameters $\kappa = 0$, $R = 0.3$, $\omega_0 = 50$.

$$C_1 = \sqrt{\frac{2\operatorname{sech}(2t/w)}{|v_1|(1-R)}}, \quad C_2 = i\sqrt{\frac{2\operatorname{sech}(2t/w)}{|v_2|(1-R)}}, \tag{46}$$

$$G_1 = \sqrt{\frac{2R\operatorname{sech}(2t/w)}{|u_1|(1-R)}}, \quad G_2 = -i\sqrt{\frac{2R\operatorname{sech}(2t/w)}{|u_2|(1-R)}}, \tag{47}$$

where $0 \leqslant R < 1$. Thus for $R = 0$ we have a soliton solution with the spectral content only at $\omega = 0$. The soliton amplitudes at $\omega = \omega_0$ start to grow as $R$ deviates from zero and for $R \to 1$ the amplitudes of the components in the subgaps at $\omega = 0$ and $\omega_0$ tend to become equal. An equivalent soliton solution with most of the energy concentrated at $\omega_0$ can be obtained on replacing $R$ with $1/R$. Thus, assuming that far from the soliton core the coherence of the Raman medium is at its maximum, we have found a family of the exponentially localized soliton solutions. The amplitudes of the fields $B_{1,2}$ calculated from Eqs. (13), (46), and (47) as functions of the parameter $v$ are shown in Fig. 2. The amplitude oscillations at $\omega_0$ cease to exist as $R \to 0$.

#### 2. Solitons with algebraically decaying tails

The minimum coherence condition (41) means that the band gap is closed and therefore the exponential localization is not possible. However, algebraically localized solutions, or rational solitons, are still possible. The second of the Eqs. (38) transforms to $\partial_x\phi = 2(1-\cos\phi)$ giving

$$\cos\phi = 1 - \frac{2}{1 + 4t^2/w^2} = \sigma, \tag{48}$$

$$\sin\phi = \frac{-4t/w}{1 + 4t^2/w^2} = Q, \tag{49}$$

$$f^2 = \frac{2}{\gamma}\frac{2}{(1+4t^2/w^2)}. \tag{50}$$

The answers for the field amplitudes in this case are obtained on replacing sech$(2t/w)$ in Eqs. (46) and (47) with $2/(1+4t^2/w^2)$.

### B. Solutions parametrized by wave number $\kappa$

In the above subsection we have zeroed the left-hand sides of Eqs. (27)–(30) by fixing $\kappa$ and as a result found solitons parametrized by velocity $v$. However, the left-hand sides can be zeroed without fixing $\kappa$, but assuming that $c_1=c_2$ and $g_1=g_2$. This can be achieved by providing $v_2=-v_1$, which requires $v=0$, and $u_2=-u_1$, which requires $\epsilon=v=0$. Thus, $v_1=u_2=-1$, $v_2=u_1=1$, $x=t$, and $\kappa$ is left free to vary. The system of equations to solve is then

$$\partial_t f = qf, \quad \partial_t q = \sigma f^2, \quad \partial_t \sigma = -qf^2. \tag{51}$$

The substitution complying with the probability constraint (5) and Eq. (26) with $\kappa \neq 0$ is

$$q = \sqrt{1-\kappa^2}\sin\phi, \quad \sigma = \sqrt{1-\kappa^2}\cos\phi, \tag{52}$$

cf. Eq. (37). The resulting equations for $f$ and $\phi$ are

$$\partial_t f = \sqrt{1-\kappa^2} f \sin\phi, \quad \partial_t \phi = \gamma f^2, \tag{53}$$

where $\gamma=c_1^2-g_1^2$. The integral of motion for Eqs. (53) is

$$\gamma f^2 + 2\sqrt{1-\kappa^2}\cos\phi = \mathcal{I}_2 = \text{const}. \tag{54}$$

Applying the boundary conditions (42) we need to integrate the equation $\partial_t\phi=-2\sqrt{1-\kappa^2}\cos\phi$ $(\mathcal{I}_2=0)$ and the equation $\partial_t\phi=2\sqrt{1-\kappa^2}(1-\cos\phi)$ $(\mathcal{I}_2=2\sqrt{1-\kappa^2})$ for the conditions (41). The first case gives us the solitons with the exponentially decaying tails

$$C_1 = \sqrt{\frac{2\,\text{sech}(2t/W)}{W(1-R)}}, \quad C_2 = i\sqrt{\frac{2\,\text{sech}(2t/W)}{W(1-R)}}, \tag{55}$$

$$G_1 = \sqrt{\frac{2R\,\text{sech}(2t/W)}{W(1-R)}}, \quad G_2 = -i\sqrt{\frac{2R\,\text{sech}(2t/W)}{W(1-R)}}, \tag{56}$$

where

$$W = \frac{1}{\sqrt{1-\kappa^2}}, \quad R = \frac{g_1^2}{c_1^2}. \tag{57}$$

The corresponding coherence and population inversion are

$$Q = -i\kappa - \sqrt{1-\kappa^2}\,th(2t/W), \tag{58}$$

$$\sigma = -\sqrt{1-\kappa^2}\,\text{sech}(2t/W). \tag{59}$$

The second case gives algebraic solitons with

$$Q = -i\kappa - \sqrt{1-\kappa^2}\frac{4t/W}{1+4t^2/W^2}, \tag{60}$$

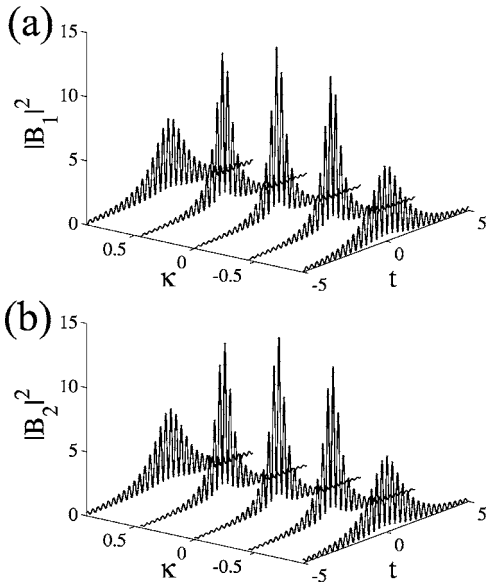


FIG. 3. Intensities $|B_{1,2}(t)|^2$ of algebraically localized solitons for different values of $\kappa$. The other parameters are $v=0$, $R=0.3$, $\omega_0=50$.

$$\sigma = \sqrt{1-\kappa^2}\left(1 - \frac{2}{1+4t^2/W^2}\right). \tag{61}$$

The field amplitudes are found in this case by replacing sech$(2t/W)$ function in Eqs. (55) and (56) with $2/(1+4t^2/W^2)$. $|B_{1,2}|$ calculated for the algebraic solitons as functions of the parameter $\kappa$ are shown in Fig. 3. $\kappa$ varying from $-1$ to $+1$ means a shift of the soliton spectrum from the lower to the upper boundary of the band gap.

## VI. NUMERICAL MODELING OF THE SOLITON PROPAGATION AND COLLISIONS

Now we will present results of the numerical modeling of the original system (1)–(4). The first series of numerical experiments we carried out was for the initial conditions given by Eqs. (46) and (47) with $R=0$. We have tested stability of these solutions for $\kappa=0$, $d_{1,2}=0$, and various values of $v$. Though no strong instabilities have been observed, we noticed that for $v>0$ the soliton experiences adiabatic changes in its velocity, while $v<0$ region is free from this effect. In order to study solutions with $R\neq 0$ we fixed $v=-0.64$, i.e., $v_1=-0.36$, $v_2=1.64$. Our choice of the dimensionless GVD coefficients is $d_1=0.0072$, $d_2=-0.0328$, which is both practically realistic and comfortably falls into the limits of validity of our slowly varying approximation giving $\omega_0=50$. Then we initialized Eqs. (1)–(4) with (46) and (47) using different values of $R$ controlling the relative energy of the fields in the two subgaps. We have found that for $R$ varying from zero to approximately 0.5 the solitons propagate stably over long distances, see Fig. 4. However, when amplitudes of the field components in the subgap at $\omega=\omega_0$ start being comparable with the ones in the subgap at $\omega=0$ $(R\to 1)$, the soliton structure becomes unstable, see Fig. 5.

Because of the approximations made in transforming Eqs.

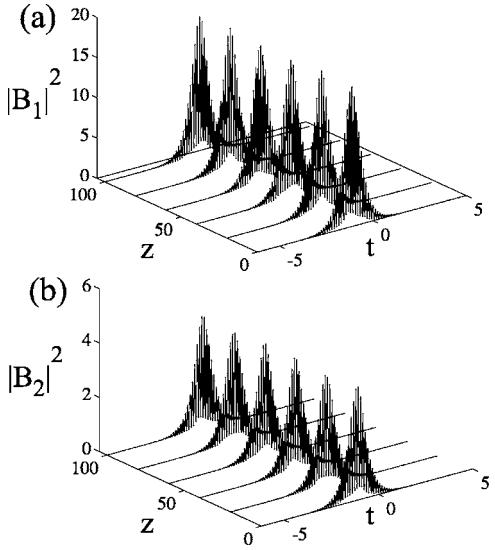


FIG. 4. $z$ evolution of the exponentially localized soliton with $R=0.3$, $\kappa=0$ as obtained from the direct numerical modeling of Eqs. (6)–(9). Parameters are $v_1=-0.36$, $d_1=0.0072$, $v_2=1.64$, $d_2=-0.0328$. The soliton is resting in the chosen reference frame.

(1)–(4) to Eqs. (14)–(19), it is not *a priori* obvious that the complete system does not impose a selection rule prescribing a certain value to $R$. Our attempts to work out possible constraints on $R$ by advancing into the next order of the perturbation theory have not given any results for the selection rule. This, however, does not completely exclude existence of the selection rule in the higher orders. Our numerical experiments indicate continuous parametrization of the soliton family with $R$, because for $R<0.5$ we have repeatedly observed stable propagation of solitons over long propagation distances with no detectable reshaping.

Since we have found, that each of the two Raman components is split into two further components by the GVD effect, see Eq. (13), the solitons with $R\neq 0$ represent the four-frequency structures. Below we demonstrate that to observe these solitons it is enough to use a two-frequency pump, which is a common setup in experiments with Raman active media [2]. We have confirmed numerically that a single frequency pump pulse is enough to excite the Raman solitons at each of the two subgaps. Thus using two laser sources detuned by $\omega_0$ one can excite the two uncoupled Raman solitons at each of the subgaps. These solitons will generally move with different group velocities and this fact can be used to our advantage. By introducing the time delay between the moments when these structures are created we have initiated their collisions. The frequently observed outcomes of these collisions have been excitations of the coupled solitons with spectrum in both subgaps. Figures 6(a) and 6(b) illustrate collision dynamics observed for the following initial conditions: $B_1=3.3\sqrt{\mathrm{sech}(t/0.25)}$ and $B_2=5\sqrt{\mathrm{sech}((t-70)/0.25)}e^{i50t}$. The initial nonsolitonic pump pulses are marked in Fig. 6 by $p_1$ and $p_2$. At the first stage of the evolution one can see the formation of the solitons $s_1$ and $s_2$. Each of those is spectrally localized at its own subgap at $\omega=0$ and $\omega=50$, respectively. For $z\approx 44$ the solitons collide and the new solitons, marked by $s_1'$ and $s_2'$, emerge from this collision. The soliton $s_1'$ remains spectrally localized inside the gap at $\omega=0$, but the second soliton $s_2'$ has two spectral

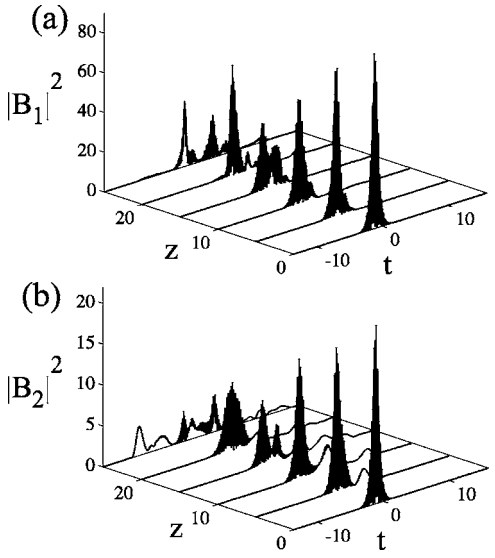


FIG. 5. The same as Fig. 4, but for $R=0.8$.

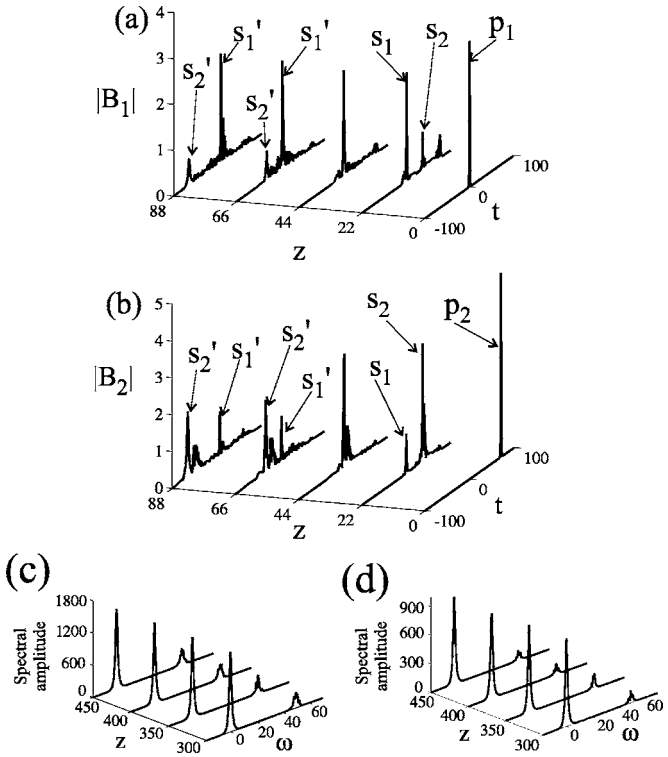


FIG. 6. (a), (b) Soliton collisions resulting from the initial conditions: $B_1=3.3\sqrt{\mathrm{sech}(t/0.25)}$, $B_2=0$ for the pulse $p_1$ and $B_1=0$, $B_2=5\sqrt{\mathrm{sech}([t-70]/0.25)}\exp(i50t)$ for the pulse $p_2$. The two solitons $s_1$ and $s_2$ formed from the initial pulses collide at $z\simeq 44$. The collision gives birth to the solitons $s_1'$ and $s_2'$. Spectra of $s_1$ and $s_2$ are localized at $\omega=0$ and $\omega=50$, respectively. Spectrum of $s_1'$ is localized around $\omega=0$, while spectra of the fields $\tilde{B}_{1,2}$ forming $s_2'$ are localized around $\omega=0$ and $\omega=50$. The spectra corresponding to $s_2'$ are shown in panels (c) and (d). (c) is the spectrum of $\tilde{B}_1$ and (d) is the spectrum of $\tilde{B}_2$.

components at each of the subgaps. This has been confirmed by cutting out the corresponding part of the time window and taking Fourier transforms of the emerging solitons, see Figs. 6(c) and 6(d) for the spectrum of $s_2'$. It has been checked that the $s_2'$-soliton propagates without spread for very long distances, see Figs. 6(c) and 6(d).

## VII. SUMMARY

We have considered the pump-Stokes interaction in a Raman medium with group velocity dispersion using the quantum mechanical description of the Raman transition. The dispersion profile with the two subgaps, which either form or do not form a complete band gap has been found in this model. An analytical technique of finding soliton families residing within the complete band gap has been developed. Estimates of the physical quantities involved and numerical modeling of the underlying partial differential equations indicate potential relevance of these structures for the experiments on the short-pulse propagation in photonic band-gap fibers filled with Raman active gases.

## ACKNOWLEDGMENTS

This work has been partially supported by EPSRC. We acknowledge interaction with C. Benton, F. Biancalana, and A. Gorbach on closely related problems.

## APPENDIX: SCALING OF EQUATIONS

In this Appendix we present details of the normalization procedure leading to Eqs. (1)–(4) and workout estimates for the scaling coefficients. We start by taking the two-field Raman equations (4.76)–(4.80) from Ref. [11] and renormalize them to the form conventional for the fiber optics literature [20]. The equations in [11] are

$$\left[\partial_z + \beta_1^{(1)}\partial_t + \frac{i}{2}\beta_1^{(2)}\partial_t^2\right]F_1 = iq_{12}\frac{\hbar\omega_1 N_0}{2\epsilon_0 c}\sigma_{21}F_2,$$

$$\left[\partial_z + \beta_2^{(1)}\partial_t + \frac{i}{2}\beta_2^{(2)}\partial_t^2\right]F_2 = iq_{12}\frac{\hbar\omega_2 N_0}{2\epsilon_0 c}\sigma_{21}^* F_1,$$

$$\partial_t\sigma_{12} + \gamma_{12}\sigma_{12} = -iq_{12}F_1^* F_2\sigma,$$

$$\partial_t\sigma + \gamma_{11}(\sigma - 1) = i2q_{12}[F_1F_2^*\sigma_{12} - F_1^*F_2\sigma_{21}],$$

where we replaced diffraction with the GVD terms and disregarded Stark shifts. $1/\beta_{1,2}^{(1)}$ are the group velocity and $\beta_{1,2}^{(2)}$ are the group velocity dispersions of the two fields. Total occupancy of the levels involved can be expressed via the coherence $\sigma_{12}$ and the population inversion $\sigma$: $4|\sigma_{12}|^2+\sigma^2=1$. The field amplitudes $F_{1,2}$ are measured in V/m and they are linked to the field amplitudes used in the context of the fiber optics [20] via $|F_{1,2}|^2=Z|A_{1,2}|/2$, where $Z=1/\epsilon_0 c$ is the impedance of the free space. Dimension of $|A_{1,2}|^2$ is $\mathrm{W/m^2}$. Introducing $Q=2\sigma_{21}=2\sigma_{12}^*$ and the Kerr nonlinearity in order to properly estimate its relative importance we have

$$i\left[\partial_z + \beta_1^{(1)}\partial_t + \frac{i}{2}\beta_1^{(2)}\partial_t^2\right]A_1 = -q_{12}\frac{\hbar\omega_1 N_0}{4\epsilon_0 c}QA_2,$$

$$i\left[\partial_z + \beta_2^{(1)}\partial_t + \frac{i}{2}\beta_2^{(2)}\partial_t^2\right]A_2 = -q_{12}\frac{\hbar\omega_2 N_0}{4\epsilon_0 c}Q^*A_1,$$

$$i\partial_t Q + \gamma_{12}Q = -q_{12}ZA_1A_2^*\sigma,$$

$$\partial_t\sigma + \gamma_{11}(\sigma - 1) = iq_{12}(Z/2)[A_1A_2^*Q^* - A_1^*A_2Q].$$

To reveal the link between the well tabulated Raman gain parameter $g_{ss}$ and the dipole moment $q_{12}$, we assume $\sigma=1$ (ground state) and $Q=iq_{12}ZT_2A_1A_2^*$. Here and below $T_2=1/\gamma_{11}$ and $T_1=1/\gamma_{12}$. Hence

$$\partial_z A_1 = -q_{12}\frac{\hbar\omega_1\bar{Z}}{2}\frac{q_{12}\bar{Z}T_2N_0}{2}A_1|A_2|^2,$$

$$\partial_z A_2 = q_{12}\frac{\hbar\omega_1\bar{Z}}{2}\frac{q_{12}\bar{Z}T_2N_0}{2}A_2|A_1|^2.$$

Steady state Raman gain is defined as growth rate of the intensity of the Stokes signal $(A_2)$ and given by $g_{ss}=q_{12}^2\hbar\omega_1\bar{Z}^2T_2N_0/2$, which has dimension of $\mathrm{mW^{-1}}$.

Now we introduce retarded time $\tau=t-z/V_+$, where $V_\pm=2/(\beta_1^{(1)}\pm\beta_2^{(1)})$ and normalize $\tau=\tau_0T$, $z=z_0\zeta$, where $T$ and $\zeta$ are dimensionless and

$$z_0 = 2\sqrt{2}\sqrt{\frac{T_2}{g_{ss}\hbar\omega_1 N_0}}, \quad \tau_0 = \frac{1}{2}z_0|\beta_1^{(1)} - \beta_2^{(1)}|.$$

Normalization for fields is

$$|A_{1,2}|^2 = \alpha|B_{1,2}|^2, \quad \alpha = \frac{1}{\tau_0}\sqrt{\frac{\hbar\omega_1 T_2 N_0}{g_{ss}}}|B_{1,2}|^2.$$

All this results in the equations

$$i\left[\partial_\zeta + s\partial_\tau + \frac{iz_0}{2\tau_0^2}\beta_1^{(2)}\partial_\tau^2\right]B_1 = -QB_2,$$

$$i\left[\partial_\zeta - s\partial_\tau + \frac{iz_0}{2\tau_0^2}\beta_2^{(2)}\partial_\tau^2\right]B_2 = -Q^*B_1,$$

$$i\left[\partial_\tau + \frac{\tau_0}{T_2}\right]Q = -B_1B_2^*\sigma,$$

$$\partial_\tau\sigma + \frac{\tau_0}{T_1}(\sigma - 1) = -\frac{i}{2}[B_1B_2^*Q^* - B_1^*B_2Q],$$

where $s=\mathrm{sgn}(V_-)$.

For our rough estimates of physical scales involved we take the density of atoms $N_0=2.5\times10^{25}\ \mathrm{m^{-3}}$, the pump frequency $\omega_1$ corresponding to the 1 $\mu$m wavelength. Choosing $D_2$ as a Raman active medium we have $g_{ss}=0.45\times10^{-11}$ m/W, $T_2\sim100$ ps. Assuming $V_-=100c$ [13] we have $z_0=0.6$ cm, $\tau_0=200$ fs, and scaling for the intensity $\alpha=4\ \mathrm{TW/cm^2}$. For the typical area of the fundamen-

tal mode of a hollow-core PBG $\simeq 50\ \mu m^2$ the above intensity corresponds to 2 MW of the peak power. Typical $|\beta^{(2)}|$ values vary from 0 to 1 $ps^2/m$, which gives us $d_{1,2} \sim z_0|\beta^{(2)}|/\tau_0^2$ varying from 0 to 0.1. The angular Raman frequency for vibrational transitions in $D_2$ is 600 rad/ps. Detuning between the two band gaps $\omega_0=50$ used in the numerical modeling corresponds to 200 rad/ps. Similar results have been obtained for detunings down to 40 rad/ps. The relaxation constants $\tau_0/T_{1,2}$ are order of $10^{-3}$ at most and have also been disregarded in Eqs. (1)–(4).


[1] M. D. Lukin and A. Imamoglu, Nature (London) **413**, 273 (2001) and references therein.

[2] A. V. Sokolov and S. E. Harris, J. Opt. B: Quantum Semiclassical Opt. **5**, 1 (2003) and references therein.

[3] A. E. Kaplan, Phys. Rev. Lett. **73**, 1243 (1994); A. E. Kaplan and P. L. Shkolnikov, J. Opt. Soc. Am. B **13**, 347 (1996).

[4] Y. Wu and L. Deng, Phys. Rev. Lett. **93**, 143904 (2004).

[5] A. V. Rybin, I. P. Vadeiko, and A. R. Bishop, Phys. Rev. E **72**, 026613 (2005).

[6] S. Ghosh, J. E. Sharping, D. G. Ouzounov, and A. L. Gaeta, Phys. Rev. Lett. **94**, 093902 (2005).

[7] F. Benabid, G. Bouwmans, J. C. Knight, P. S. J. Russell, and F. Couny, Phys. Rev. Lett. **93**, 123903 (2004).

[8] S. Ghosh, A. R. Bhagwat, C. K. Renshaw, S. Goh, A. L. Gaeta, and B. J. Kirby, Phys. Rev. Lett. **97**, 023603 (2006).

[9] D. G. Ouzounov, F. R. Ahmad, D. Müller, N. Venkataraman, M. T. Gallagher, M. G. Thomas, J. Silcox, K. W. Koch, and A. L. Gaeta, Science **301**, 1702 (2003); F. Luan, J. C. Knight, P. S. J. Russell, S. Campbell, D. Xiao, D. T. Reid, B. J. Mangan, D. P. Williams, and P. J. Roberts, Opt. Express **12**, 835 (2004).

[10] D. V. Skryabin, A. V. Yulin, and F. Biancalana, Phys. Rev. E **73**, 045603(R) (2006).

[11] A. C. Newell and J. V. Moloney, *Nonlinear Optics* (Addison-Wesley, Redwood City, 1992).

[12] F. Y. F. Chu and A. C. Scott, Phys. Rev. A **12**, 2060 (1975); G. S. McDonald, Opt. Lett. **20**, 822 (1995); M. Scalora, S. Singh, and C. M. Bowden, Phys. Rev. Lett. **70**, 1248 (1993); J.-G. Caputo and A. Maimistov, Phys. Rev. E **71**, 036601 (2005).

[13] D. V. Skryabin, F. Biancalana, D. M. Bird, and F. Benabid, Phys. Rev. Lett. **93**, 143907 (2004).

[14] T. M. Makhviladze and M. E. Sarychev, Sov. Phys. JETP **44**, 471 (1977).

[15] A. V. Sokolov, S. J. Sharpe, M. Shverdin, D. R. Walker, D. D. Yavuz, G. Y. Yin, and S. E. Harris, Opt. Lett. **26**, 728 (2001).

[16] D. J. Kaup, Physica D **6**, 143 (1983); H. Steudel, *ibid.* **6**, 155 (1983).

[17] J. R. Kuklinski, U. Gaubatz, F. T. Hioe, and K. Bergmann, Phys. Rev. A **40**, R6741 (1989); N. V. Vitanov, K. A. Suominen, and B. W. Shore, J. Phys. B **32**, 4535 (1999).

[18] R. Grimshaw and B. A. Malomed, Phys. Rev. Lett. **72**, 949 (1994).

[19] B. Z. Essimbi, L. Ambassa, and T. C. Kofane, Physica D **106**, 207 (1997).

[20] G. P. Agrawal, *Nonlinear Fiber Optics* (Academic Press, San Diego, 2001).